

Zeitschrift: IABSE reports = Rapports AIPC = IVBH Berichte
Band: 78 (1998)

Artikel: Development of Wing Segments
Autor: Konda, Toru / Nomoto, Toshi / Mito, Kenji
DOI: <https://doi.org/10.5169/seals-59035>

Nutzungsbedingungen

Die ETH-Bibliothek ist die Anbieterin der digitalisierten Zeitschriften auf E-Periodica. Sie besitzt keine Urheberrechte an den Zeitschriften und ist nicht verantwortlich für deren Inhalte. Die Rechte liegen in der Regel bei den Herausgebern beziehungsweise den externen Rechteinhabern. Das Veröffentlichen von Bildern in Print- und Online-Publikationen sowie auf Social Media-Kanälen oder Webseiten ist nur mit vorheriger Genehmigung der Rechteinhaber erlaubt. [Mehr erfahren](#)

Conditions d'utilisation

L'ETH Library est le fournisseur des revues numérisées. Elle ne détient aucun droit d'auteur sur les revues et n'est pas responsable de leur contenu. En règle générale, les droits sont détenus par les éditeurs ou les détenteurs de droits externes. La reproduction d'images dans des publications imprimées ou en ligne ainsi que sur des canaux de médias sociaux ou des sites web n'est autorisée qu'avec l'accord préalable des détenteurs des droits. [En savoir plus](#)

Terms of use

The ETH Library is the provider of the digitised journals. It does not own any copyrights to the journals and is not responsible for their content. The rights usually lie with the publishers or the external rights holders. Publishing images in print and online publications, as well as on social media channels or websites, is only permitted with the prior consent of the rights holders. [Find out more](#)

Download PDF: 16.01.2026

ETH-Bibliothek Zürich, E-Periodica, <https://www.e-periodica.ch>

Development of Wing Segments

Toru Konda

Doctor of Engineering,
Professor, Engineering Department,
Tokyo Municipal University
Tokyo, Japan

Toshi Nomoto

Doctor of Engineering
Technological Laboratory,
Nishimatsu Construction Co., Ltd.
Kanagawa, Japan

Kenji Mito

Engineer, Civil Engineering
Civil Engineering Design Department,
Nishimatsu Construction Co., Ltd.
Tokyo, Japan

Hiroshi Yamazaki

M.E.
Technological Laboratory,
Nishimatsu Construction Co., Ltd.
Kanagawa, Japan

Abstract

Wing segments are developed aiming the efficient moment transfer at the joints of shield lining to maintain necessary lining stiffness in very soft ground where enough passive pressure is not mobilized, and to reduce the cost of joints. In developing wing segments full-scale loading tests have been conducted. The test results show that maintaining the shearing stiffness at the end of wing joint could attain sufficient moment transfer at joints. Unlike ordinary segments, the moment transfer by bolts is not significant and the number and size of bolts could be reduced in the segments.

1. Introduction

In Japan shield tunnels are often constructed in soft ground. Accordingly enough passive pressure is not mobilized and a large bending moment occurs in the lining. For ordinary rectangular segments, lining stiffness is covered by the longitudinal joint positions are not continuous for tunnel axis (hereafter referred to as staggered pattern). To maintain strength of the lining and prevent joint opening are needed, however, heavily reinforced and expensive joints are required.

The authors developed a wing segment that reduces the number of bolts used and decreases the bolt diameter by modifying the shape of the segment pieces. The longitudinal joints have extension part in circumferential direction that equal about half width of the segment, and tenons that we call shearing keys are placed in the joint surface. Wing segment can be attained efficient moment transfer caused by shearing stiffness, and sufficient ring strength and ring stiffness in very soft ground. This paper presents a basic construction of the wing segment and the results of the loading tests conducted with full-scale segments (5300mm external diameter, 1200mm width, 250mm thickness, six pieces).



2. Basic Construction of Wing Segments

2.1 Shape

Figure 1 shows the basic construction of wing segments. The segments are made up of the "main section" and "wing sections." The longitudinal joint surfaces of the segments have shearing keys, so that shear resistance force can be transmitted effectively.

2.2 Mechanism of Bending Moment Transfer

Figure 2 shows the structural transmission mechanism of bending moment in the wing segment joint. The bending moment that works on the joint (M) is divided into that which works on the bolts (M_b) and that which works on the base of the wing section (M_w). M_w is the sum of the bending moment that works on the shearing key ($M_s = S_j \times L$) and M_b .

$$\begin{aligned}
 M &= M_b + M_w \\
 &= M_b + (M_s + M_b) = 2M_b + M_s \\
 M &: \text{Bending moment that works on the joint.} \\
 M_b &: \text{Bending moment that works on the bolts.} \\
 M_w &: \text{Bending moment that works on the base of the wing section.} \\
 M_s &: \text{Bending moment that works on the shearing key} (= S_j \times L). \\
 S_j &: \text{Shearing force that works on the shearing key.} \\
 L &: \text{Wing length}
 \end{aligned}$$

M_s and M_b resist the bending moment M that works on the joint. Therefore, by placing a higher percentage of the bending moment on the shearing key the burden placed on the bolts can be reduced. In other words, the number of bolts or their diameter can be reduced.

Theoretical analysis was conducted by using a cantilever model as shown in Figure 3. A model was constructed in which both wing sections face each other and are joined by rotation springs and shearing springs.

The cross section of a single subway tunnel was used for the analysis. The relations between the wing length and the bending moment percentage on the bolt, the base of the wing section and the shearing key and between the wing length and equivalent rotation stiffness that converted ordinary joint were calculated. The results of the analysis are shown in Figure 4. The bending moment percentages on the each section are shown below.

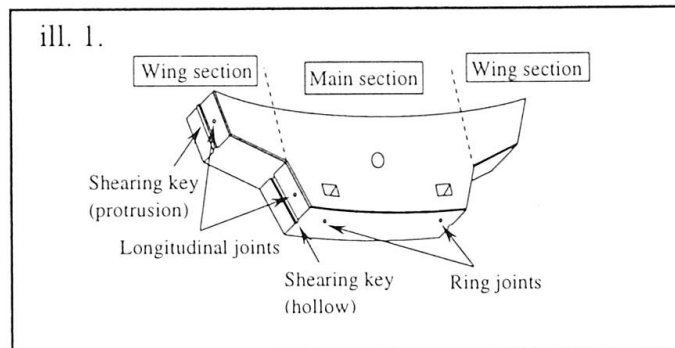


Fig. 1 Basic Construction of Wing Segments

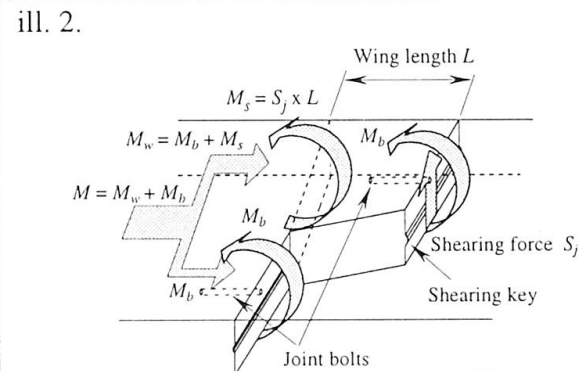


Fig. 2 Mechanism of Bending Moment Transfer by Shearing Force

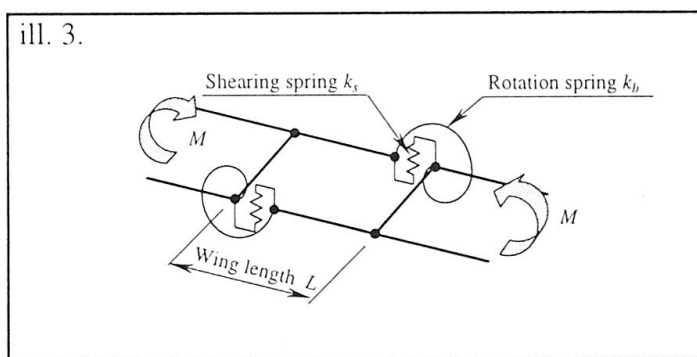


Fig. 3 Cantilever Model

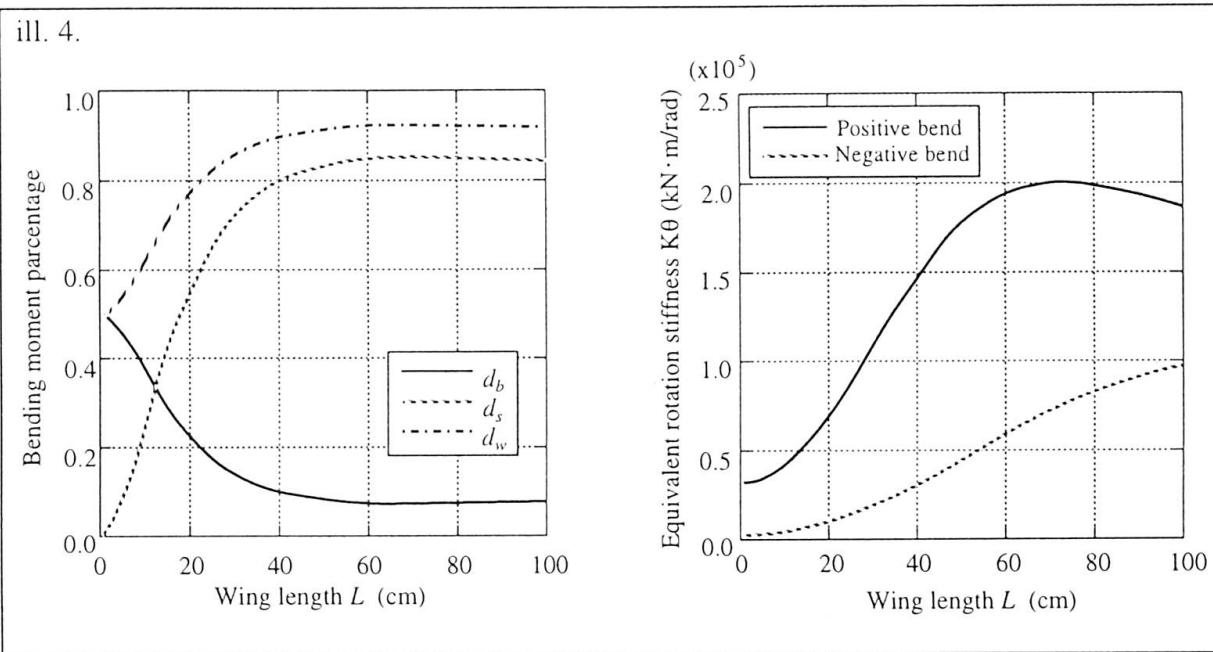


Fig. 4 Wing Length (L) Sensitivity Analysis

$$db = Mb/M$$

$$dw = Mw/M$$

$$ds = Ms/M$$

db : Bending moment percentage on the bolts.

dw : Bending moment percentage on wing section base.

ds : Bending moment percentage on the shearing key.

Longer wing sections are better to reduce the burden on the bolts. The analysis showed that the bending moment percentages and equivalent rotation stiffness became changeless when the wing length exceeded 60 centimeters. Therefore, the wing length in the full size segment load presence tests was set at 60 centimeters.

3. Loading Tests Using Full-Scale Segments

The aim of developing wing segments was to attain strength and stiffness equal to or higher than staggered pattern rectangular segments even if wing segments' longitudinal joint positions were continuous for tunnel axis (hereafter referred to as inline pattern). A series of the loading tests using full-scale segments was carried out in order to investigate this. Figure 5 shows the section items for the test piece. The materials used are shown in Table 1.

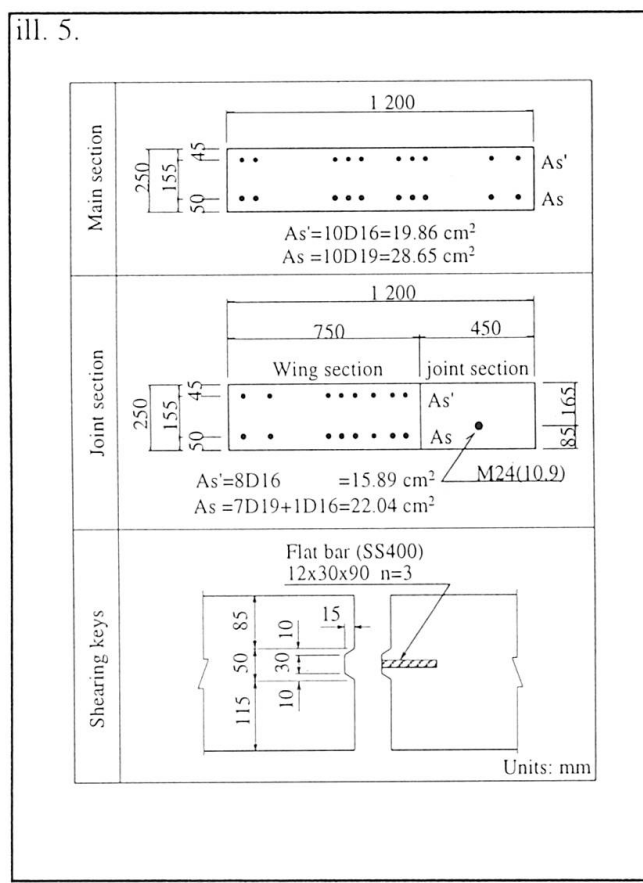


Fig. 5 Cross Sections of the Test Piece



3.1 Shearing Key Shearing Test

3.1.1 Purpose of the test

To obtain the shearing spring constant and confirm shearing strength of the shearing key on the joint surface.

3.1.2 Testing Method

Figure 6 shows an outline of the testing method. Tests were conducted on the loading conditions that occurred positive bending moment (Case 1) and negative bending moment (Case 2) at the joint.. Axial force was set at 441 kN per segment width and 221 kN per longitudinal joint surface to comply with the joint bending test and ring loading test to be described later.

3.1.3 Test Results

1) Shearing strength

Table 2 shows the test results. Because compression caused cracks early in Case 2, the collapse load was smaller than for Case 1. However, it was found that the shearing key had sufficient shearing strength because the collapse load is greater than the design ultimate load.,

2) Shearing stiffness

Figure 7 shows the relations between presence load and shearing deformation. The design values in the figure do not take friction resistance caused by axial force into consideration. Although shearing cracks resulted after the allowable load was exceeded, it can be seen that there are no major changes in shearing stiffness even after the cracks appear. If the shearing stiffness of wing segments are overestimated, the bolts will be underestimated and safety problems will develop. The actual shearing stiffness measured was larger than shearing spring constant design values calculated after considering the stiffness of the concrete and the shear reinforcement. This showed that the design value of the shearing spring constant was safe value.

Table 1.

Material	Strength properties / Units: N/mm ²	
Concrete	Standard design strength	$\sigma_{ck} = 48$
	Allowable compressive stress	$\sigma_{ca} = 17$
	Allowable shearing stress	$\tau_{ca} = 0.74$
Reinforcement	Yield stress	$\sigma_{sy} = 345$
	Allowable compressive stress	$\sigma_{sa} = 200$
	Allowable tensile stress	$\sigma_{ta} = 200$
Bolts	Yield stress	$\sigma_{sy} = 940$
	Allowable tensile stress	$\sigma_{ta} = 300$

Table 1 Materials

ill. 6.

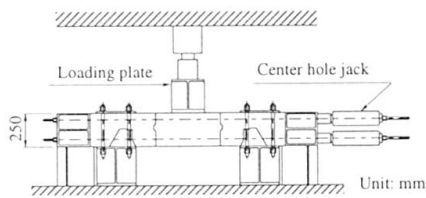


Fig. 6 Shearing Test Outline

Table 2.

		Case 1	Case 2
Design values	Allowable load P_a (kN)	263	257
	Final load P_{ru} (kN)	555	512
Test values	Collapse load P_u (kN)	842	669
	Safety factor F_s ($=P_u/P_a$)	3.21	2.61

Table 2 Shearing Test Results

ill. 7.

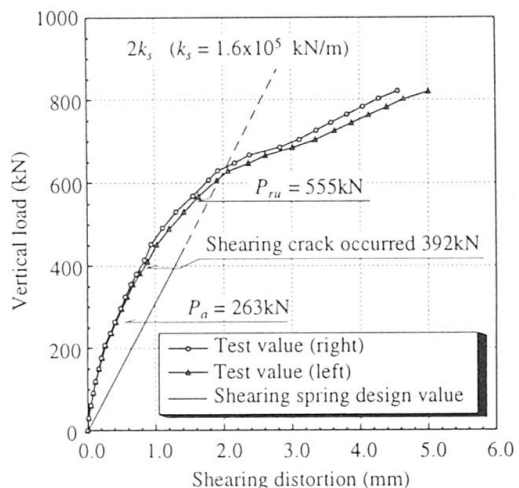


Fig. 7 Relations Between Load and Shearing Distortion

3.2 Joint Bending Test

3.2.1 Purpose of the test

To confirm the mechanism of bending moment transfer by the shearing key, and to verify the strength and stiffness of the joint.

3.2.2 Testing Method

Figure 8 shows an outline of the testing method. The load was applied so that the ratio of the bending moment and the axial force was constant until the allowable bending moment. After the allowable bending moment was exceeded, the load was applied so that the axial force remained constant and the bending moment increased. The section forces at the allowable bending moment were set at 368 kN/m for the axial force and 90.7 kNm/m for the bending moment to comply with the final proof stress confirmed through the ring load test.

3.2.3 Test Results

Table 3 shows the test results. The bending moment at collapse was about the same as the design final bending moment. This is believed to be the result of sufficient transmission of the bending moment by the shearing key (shearing resistance (S) x Wing length (L)).

3.3 Ring Loading Test

3.3.1 Purpose of the test

To investigate the strength and deformation properties of the wing segment ring under the axial force.

3.3.2 Testing Method

Figure 9 shows an outline of the testing method. The load was applied so that the ratio of the bending moment and the axis force were constant until the allowable bending moment. Bending moment was applied by placing concentrated loads (P_v and P_h) on the vertical and horizontal directions of the segment. Part-1, 3 were placed on the ring so that the maximum positive bending moment worked on the main section and the maximum negative bending moment worked on the wing sections. Part-2 was placed opposite to Part-1, 3. In the test concentrated loads (P_v and P_h) were introduced proportionately until the design bending moment, but in the final load condition test P_h was set at 0.

ill. 8.

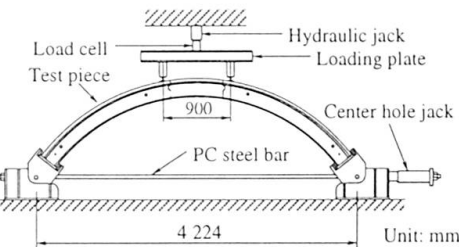


Fig. 8 Joint Bending Test Outline

Table 3

(Units: kNm/m)		
Design values	Allowable bending moment M_a	90.7
	Final bending moment M_{ra}	178
Test values	Bending moment at collapse M_u	180
	Safety factor $F_s (=M_u/M_a)$	1.99

Note: An axis force of 368 kN was used for the joint bending test.

Table 3 Joint Bending Test Results

ill. 9.

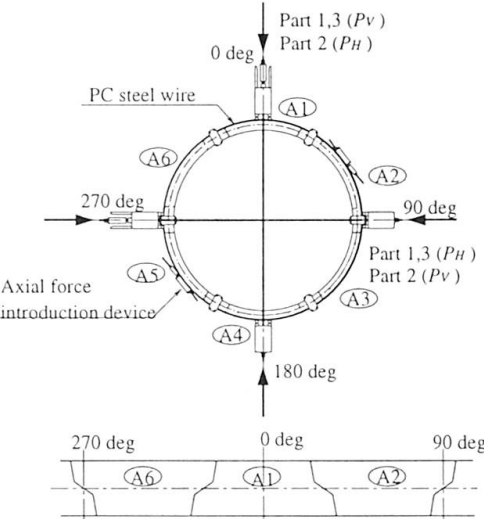


Fig. 9 Ring Loading Test Outline



3.3.3 Test Results

Figure 10 shows the relations between the load and convergence of the segment ring in Case 3. The specifications of the bolts in the wing segment were smaller than those for conventional bolts. At the allowable bending moment level the ring stiffness was equivalent to or greater than that of the rectangular segment staggered pattern ring calculations in the structural analysis. This shows that the bending moment is transmitted effectively by the shearing keys, and that stiffness has been improved. Also the bending moment distribution in the main section of the segment calculated from the strain measurements on the steel reinforcements is equivalent to the distribution in uniform stiffness rings. Therefore, it was confirmed that wing segments can be designed as uniform stiffness rings ignoring the joint.

Table 4 shows a summary of the final proof stress results. The bending moment at the end of tests was higher than the design final bending moment of rectangular segment staggered pattern rings. This confirms that wing segments can provide sufficient proof stress even inline pattern construction. In each test case bending collapse occurred at the position where the maximum positive bending moment was occurred.

4. Conclusions

The conclusions that resulted from the full size segment loading tests were as follows:

- 1) The wing segment feature of transmitting bending moment with shearing stiffness was confirmed, and it was verified that the number of bolts or their diameter can be reduced.
- 2) It was verified that ring proof stress and ring stiffness equal to or greater than that for rectangular segment staggered pattern rings could be achieved with inline pattern construction using fewer bolts or bolts with smaller specifications.
- 3) In joint bending tests where axial force was introduced, joint behavior similar to that in the ring loading test was confirmed. Therefore, it was confirmed that this simple test could sufficiently replace the ring loading tests.

Reference

- 1) Hiroshi Yamazaki, Toshi Nomoto and Kenji Mito; "Wing Segment Development"; "Tunnels and Underground," vol. 28, no. 5, pp. 387-395 (May 1997)

ill. 10.

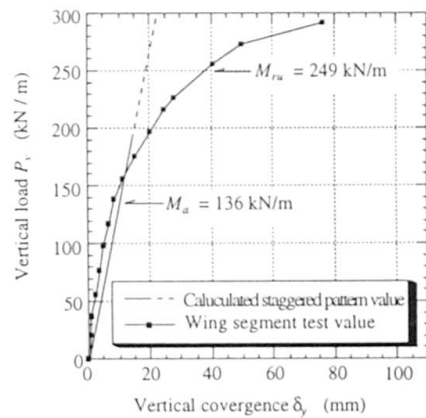


Fig. 10 Relations Between Vertical Loads and Vertical Convergence

Table 4.

		Part 1	Part 2	Part 3
	Maximum positive bend	Main section	Joint	Main section
Design values	M_a (kNm/m)	110	90.7	110
	M_u (kNm/m)	200	178	200
Test values	M_u (kNm/m)	209	212	243
	Safety factor F_s ($= M_u / M_a$)	1.90	2.34	2.22

Table 4 Ring Loading Test Results